Chemosphere 194 (2018) 657–665

Contents lists available at ScienceDirect

Chemosphere

journal homepage: www.elsevier.com/locate/chemosphere

Transcriptome analysis reveals novel insights into the response to Pb exposure in *Phanerochaete chrysosporium*

Chao Huang [a], Rongzhong Wang [a], Guangming Zeng [a, *], Danlian Huang [a, **], Cui Lai [a], Jiachao Zhang [b], Zhihua Xiao [c], Jia Wan [a], Piao Xu [a], Xiaomin Gong [a], Wenjing Xue [a], Xiaoya Ren [a]

[a] College of Environmental Science and Engineering, Hunan University, Key Laboratory of Environmental Biology and Pollution Control (Hunan University), Ministry of Education, Changsha 410082, PR China
[b] College of Resources and Environment, Hunan Agricultural University, Changsha 410128, PR China
[c] College of Bioscience and Biotechnology, Hunan Agricultural University, Changsha 410128, PR China

HIGHLIGHTS

- Pb affected fungal growth and Pb accumulation in a dose- and time-dependent manner.
- cDNA-AFLP analysis revealed the Pb-responsive genes in *P. chrysosporium*.
- Genes involved in ion binding, energy and signal transduction were altered.
- qRT-PCR analysis of six Pb-responsive genes validated the cDNA-AFLP result.

GRAPHICAL ABSTRACT

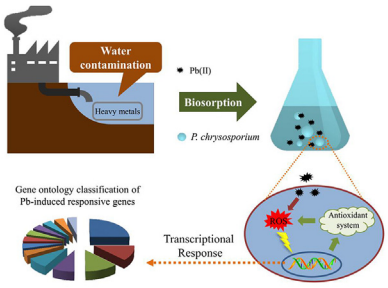

ARTICLE INFO

Article history:
Received 19 October 2017
Received in revised form
30 November 2017
Accepted 8 December 2017
Available online 9 December 2017

Handling Editor: Frederic Leusch

Keywords:
Phanerochaete chrysosporium
Pb
cDNA-AFLP
TDFs
Gene expression

ABSTRACT

Metals released into the environment continue to be of concern for human health. Using white-rot fungi as biosorbents for heavy metals removal is an attractive alternative owing to its good performance and low cost. However, the molecular mechanism underlying heavy metal tolerance in white-rot fungi has not yet been fully elucidated. This study identified and analyzed the lead (Pb)-induced transcriptional changes in *Phanerochaete chrysosporium*, a well-known heavy metal hyperaccumulating white-rot fungus. The results confirmed its outstanding ability in Pb tolerance and effective defense system. By comparative analysis of gene expression profiles obtained from cDNA-amplified fragment length polymorphism (cDNA-AFLP), we isolated 43 transcript-derived fragments (TDFs) differentially regulated by Pb exposure in *P. chrysosporium*, and 23 TDFs presented significant similarities to genes encoding known or putative proteins which belong to different functional categories involving ion binding, energy and carbohydrate metabolism, and signal transduction. The detailed characterization of these Pb-responsive genes was presented and the expression patterns of some interesting genes were validated by quantitative RT-PCR. This work provides the first evidence of Pb-responsive genes along with their putatively functional annotations in *P. chrysosporium*, which may help to understand the mechanism underlying heavy metal accumulation and tolerance in *P. chrysosporium*.

* Corresponding author.
** Corresponding author.
E-mail addresses: zgming@hnu.edu.cn (G. Zeng), huangdanlian@hnu.edu.cn (D. Huang).

https://doi.org/10.1016/j.chemosphere.2017.12.046
0045-6535/

1. Introduction

Heavy metal pollution has aroused significant concerns since it can cause adverse health effects on humans, notably reproductive abnormalities, fetal death, and neurological and behavioral disorders (Gong et al., 2017; Huang et al., 2016b, 2017c; Zeng et al., 2013a,b). Among the heavy metals, lead (Pb) requires special attention for its high toxicity and long-term persistence in biological systems (Jacobs et al., 2002; Lai et al., 2016; Neale et al., 2017; Wan et al., 2018). During the past few decades, various methods including chemical precipitation, ion-exchange, adsorption, membrane filtration and electrochemical reduction/precipitation have been devoted to the heavy metal removal from wastewater (Wang et al., 2013, 2015a,b; Yu et al., 2017; Zhang et al., 2014, 2016). Biosorption is regarded as a highly efficient, cost-effective and eco-friendly solution and thus becomes a potential alternative for the removal or recovery of heavy metals from the contaminated sites (Ren et al., 2018; Xu et al., 2012a; Yang et al., 2010). *Phanerochaete chrysosporium*, a well-known heavy metal biosorbent, has been devised for the removal of Pb with outstanding bioaccumulation ability (Xu et al., 2012b, 2016). Simultaneously, our previous study confirmed that *P. chrysosporium* could survive up to 400 mg L^{-1} of Pb, which indicated that this fungus had an excellent tolerance to Pb and must have evolved an efficient defense mechanism in the alleviation of Pb toxicity (Li et al., 2015).

To date, many studies have characterized the mechanisms underlying heavy metal detoxification in white-rot fungi, especially in *P. chrysosporium* (Petr, 2003; Zhao et al., 2015). For instance, it is known that enzymatic antioxidants like superoxide dismutase (SOD) and non-enzymatic antioxidants such as glutathione play an important part in heavy-metal detoxification in *P. chrysosporium* (Chen et al., 2014; Xu et al., 2016). *P. chrysosporium* not only exhibits an admirable accumulation capacity of Pb, but also can alleviate Pb-induced oxidative stress via its highly defensive behavior including an elevation in SOD activity and glutathione accumulation (Huang et al., 2017a). Besides, the organic acids, especially oxalate, in the extracellular polymeric substances correlate well with Pb level and tend to be the major metal chelator produced by *P. chrysosporium* (Li et al., 2015). However, little attention has been paid to the global molecular response of this fungus to heavy metal. The heavy metal-regulated genes as well as their role in hyper-accumulation and tolerance in *P. chrysosporium* are still completely unclear.

The recent development of molecular biological technologies, including microarray and next generation sequencing (NGS), has allowed a simultaneous evaluation of multiple biological responses (Jiang et al., 2016; Vidal-Dorsch et al., 2016). The application of these approaches to ecotoxicology can provide rich data and is advantageous in identifying causative stressors and sources (Brockmeier et al., 2016; Jia et al., 2017). However, microarray analysis requires prior sequence information and NGS is always expensive. cDNA-amplified fragment length polymorphism (cDNA-AFLP), acting as a sensitive, efficient and reproducible RNA fingerprinting technique, has been widely used in isolating and identifying the differentially expressed genes under certain stress condition (Hiki et al., 2017; Oberholster et al., 2016). It is cost-effective and does not require prior sequence information compared with microarray or NGS, and has been widely applied in identification of novel genes in various organisms (Georgieva et al., 2012; Vuylsteke et al., 2007). For example, it has been successfully applied to analysis of Mn-regulated genes in fungus *Ceriporiopsis subvermispora* (Gutiérrez et al., 2008) and identification of Cd− and Mn-regulated genes in plants (Ruytinx et al., 2011; Zhou et al., 2017). Therefore, we employ the cDNA-AFLP technology to identify the differentially expressed genes in *P. chrysosporium* in response to Pb exposure.

This study aimed to characterize the biochemical signals associated with the behavior of *P. chrysosporium* by transcriptome assay, identifying the genes activated or repressed responding to Pb exposure. Apart from the evaluation of Pb exposure on the fungal growth and fungal ability in Pb accumulation, the differentially expressed cDNA fragments in *P. chrysosporium* were isolated, sequenced, and the corresponding functions and their expression patterns were investigated and analyzed. The expression patterns of some interesting genes were validated by quantitative RT-PCR analysis.

2. Materials and methods

2.1. Strain and inoculation

The *P. chrysosporium* strain (BKM-F-1767) was purchased from China Center for type Culture Collection (Wuhan, China). The strain was grown on potato dextrose agar plates at 37 °C for 48 h to achieve spore production. The spore suspensions were prepared by scraping spores from plates and blending them in sterile water, and its concentration was adjusted to 2.0×10^6 CFU mL^{-1} according to our previous work (Huang et al., 2016a). Spore suspensions (2 mL) were inoculated into 100 mL of sterile potato dextrose broth and incubated at 30 °C with shaking (150 rpm).

2.2. Pb exposure test and biomass determination

After 41 h incubation, cells reached the exponential growth phase based on our previous results (Huang et al., 2017a), $Pb(NO_3)_2$ solution was then added to the liquid medium and the final Pb concentrations were controlled at 0, 50, and 400 mg L^{-1}. The fungus cultured without Pb was defined as the control sample. Each treatment was carried out in three replicates. The mycelia were harvested after Pb exposure for 0, 2, 8, and 24 h by filtration and washing twice with sterile water, and stored at −80 °C after frozen in liquid nitrogen. For biomass determination, the mycelia were collected at selected intervals and measured after washing twice with sterile water and drying at 80 °C for 24 h.

2.3. RNA extraction and cDNA synthesis

Total RNA was extracted from about 50 mg of the frozen mycelia using Trizol reagent (Invitrogen) as described previously (Huang et al., 2017b). The quality and quantity of RNA was monitored by 1% agarose gel electrophoresis and spectrophotometric analysis (Eppendorf BioPhotometer Plus, Hamburg, Germany). After removing the genomic DNA by using DNase I (Promega) at 37 °C for 30 min and purification, the first-strand cDNA was synthesized from 2 μg of total RNA using RevertAid™ First Strand cDNA Synthesis Kit (Fermentas). The synthesis of double-stranded cDNA was performed by adding *Escherichia coli* RNase H, *E. coli* DNA Ploymerase I and T4 DNA Polymerase (Promega), and terminated by EDTA (pH 8.0). After cDNA synthesis, samples were purified by phenol/chloroform extractions and checked by agarose gel electrophoresis.

2.4. cDNA-AFLP analysis

The cDNA-AFLP analysis was performed as described previously with slight modifications (Hiki et al., 2017; Vos et al., 1995). About 0.5 μg of double-stranded cDNA was digested first with *Eco*RI (Fermentas) at 37 °C for 3 h followed by *Mse*I (Fermentas) at 65 °C for 3 h, and then heated to 80 °C for 10 min to inactivate the enzymes. The resulting restricted fragments were ligated to the *Eco*RI and *Mse*I adaptors using T4 DNA ligase (NEB) at 16 °C overnight.

Table 1
Primers used for cDNA-AFLP and qRT-PCR analysis.

Adapters/primers	Sequences (5'→ 3')	
cDNA-AFLP primer		
Adapters	*EcoR I adapter-F*	*EcoR I adapter-R*
	CTCGTAGACTGCGTACC	AATTGGTACGCAGTCTAC
	Mse I adapter-F	*Mse I adapter-R*
	GACGATGAGTCCTGAG	TACTCAGGACTCAT
Pre-amplication primer	*EcoR I + A*	*Mse I + C*
	GACTGCGTACCAATTCA	GATGAGTCCTGAGTAAC
Amplification primers	*EcoR I + NNN*	*Mse I + NNN*
	EcoR I + AAC	Mse I + CAA
	EcoR I + ACC	Mse I + CTT
	EcoR I + AGC	Mse I + CAT
	EcoR I + AGG	Mse I + CAC
	EcoR I + CCA	Mse I + ATC
	EcoR I + TAA	Mse I + ACT
	EcoR I + CAG	Mse I + CTC
		Mse I + AGT
		Mse I + ATA
qRT-PCR primers		
TDF 1-1	TGGAGCGGTCAGTTTGAG	TGTCCATCACAGCCACTAT
TDF 12-1	GTGGTGGTCAAGACAATTACGA	GACGCCGCAACCTTTGTT
TDF 15-1	CATCCTCCTGACAATCTT	TCTCCAACATAGCCTTAG
TDF 42-1	GTATGAGCACTGTCAGAGA	AAAGCGTTTGGAGGAGTA
TDF 45-1	TCTCTAACCAGGCTATGA	CTGTTTGGAAAGACTGAAG
TDF 47-1	AAGCAACTACCGTCTACT	CGAAAGTGAAATGGGTTATC
β-actin	ACTCTGGTGATGGTGTCTC	TGTGGTGTTGAAGGGGTAA

Preamplification was performed using 25 μL of 2 × PCR Master Mix (Fermentas), 5 μL of ligation mixture, 0.4 μM pre-amplification primers of *Eco*RI and *Mse*I (Table 1), and nuclease-free water to a total volume of 50 μL. PCR conditions were: an initial hold of 2 min at 94 °C, 28 cycles composed of 1 min at 94 °C, 1 min at 56 °C and 1 min at 72 °C, and a final hold of 5 min at 72 °C. The pre-amplified products were checked by 1% agarose gel electrophoresis and diluted 50-fold with nuclease-free water. Selective amplification was performed using 10 μL of 2 × PCR Master Mix (Fermentas), 1 μL of preamplified product, 0.2 μM selective amplification primers of *Eco*RI and *Mse*I (Table 1), and nuclease-free water to a total volume of 20 μL. The PCR amplification was conducted using a touch-down program as follows: an initial hold of 2 min at 94 °C, followed by 12 cycles composed of 30 s at 94 °C, 30 s at 65 °C (−0.7 °C per cycle) and 1 min at 72 °C, followed by 23 cycles composed of 30 s at 94 °C, 30 s at 56 °C and 1 min at 72 °C, and a final hold of 10 min at 72 °C. The amplification products were mixed with formamide/bromophenol blue loading buffer and denatured for 5 min at 95 °C. The denatured samples were separated in a 6% denaturing polyacrylamide sequencing gel at 70 W constant power for 2.5 h, the resultant gel was stained with silver nitrate.

2.5. Isolation, sequencing and annotation

The transcript derived fragments (TDFs) of interest that exhibited different expression patterns were excised from the gels and used as the template for re-amplification in the same conditions as that used for the selective amplification. The re-amplification products were checked by 2% agarose gel electrophoresis and purified by an agarose gel recovery kit (Solarbio, China). After ligation to pGEM-T EASY vector (Promega) and transformation in *Escherichia coli* (DH5α), the TDFs fragments (three clones for each one) were sequenced on an automated ABI-3730 sequencer (Applied Biosystems) at PersonalBio (Shanghai Personal Biotechnology Co. Ltd, Shanghai, China). After removing the vector sequence, the TDFs sequences were analyzed by Blast2GO software v2.0 (Conesa et al., 2005) for functional annotation. In general, the sequences were analyzed by running BlastX similarity searches against the NCBI non-redundant protein database with a cut off E-value of 10^{-3}, then GO mapping and annotation with the default value. InterProScan was performed to improve annotation ability and the resulted GO terms were merged to annotation. If no significant homology result was obtained, the sequence was further analyzed using BlastN against the NCBI expressed sequence tag database so as to identify UniGene sequence clusters. Functional proteins associated with UniGene clusters were then used for annotation. After annotation, the differentially expressed transcripts were grouped according to the upper level GO terms for biological process, molecular function, and cellular component.

2.6. qRT-PCR analysis

To validate the results obtained from cDNA-AFLP, qRT-PCR was conducted for some TDFs that displayed differentially expression patterns. Total RNA extraction and first-strand cDNA synthesis were conducted the same as presented above. β-actin was selected as the housekeeping gene used for normalization. Primers (Table 1) for qRT-PCR were designed using Primer Premier 5.0 (PREMIER Biosoft, Canada). The qPCR was performed in an iQ5 system (Bio-Rad, Hercules, CA) using Power SYBR Green Kit (Takara, Dalian, China). The qPCR conditions were 95 °C, 2 min; 40 cycles of 95 °C for 15 s and 55 °C for 30 s; and hold at 72 °C for 10 min. Samples for qPCR were run in three biological replicates and three technical replicates. The target gene expression was normalized relative to β-actin according to the method of Livak and Schmittgen (2001).

2.7. Statistical analyses

The statistical comparisons were performed by one-way analysis of variance (ANOVA) and Fisher's least significance difference test (LSD). For the analysis of cDNA-AFLP profiles, a matrix was constructed based on the presence or absence of the differentially expressed bands on the gels, which were marked as 0 (band absent or faint), 1 (band present), or 2 (band bold). Each treatment lane was used as a variable, and each transcript as an observation. An average linkage hierarchical cluster analysis (HCA) was conducted based on the correlation matrix to describe groups of TDFs co-expressed or putatively related to common metabolic pathways. The statistical analyses were performed using SPSS v18.0 and $P < 0.05$ was deemed significant.

3. Results

3.1. Fungal growth and Pb accumulation

To determine the potential toxicity of Pb to *P. chrysosporium*, the present work evaluated the effect of Pb exposure time and concentration on the growth and metal accumulation of *P. chrysosporium*. The results showed that 50 mg L^{-1} of Pb exposure did not pose a severe threat to *P. chrysosporium* during the 24-h time period as evidenced by the sustained increase in biomass (Fig. 1a). Pb accumulation increased with the exposure time, which presented a faster increase before initial 8 h and relatively slower thereafter compared with biomass. No significant difference was found between the biomass of the control and the treatment with 50 mg L^{-1} Pb for 8 h (Fig. 1b). However, high concentration of Pb (400 mg L^{-1}) caused a significant inhibition in the growth of *P. chrysosporium* although it could survive in such a condition. In addition, *P. chrysosporium* displayed a high ability to accumulate Pb and it presented to follow a dose-dependent trend. The exposure to 400 mg L^{-1} Pb for 8 h caused 160% increase in Pb accumulation with respect to 50 mg L^{-1} Pb.

3.2. Detection of differentially expressed fragments by cDNA-AFLP

Different Pb concentrations (0, 50, and 400 mg L^{-1}) and exposure time (0, 2, 8, and 24 h) were selected to identify the differentially expressed genes in *P. chrysosporium* by cDNA-AFLP. By using 63 primer combinations, a total of about 300 TDFs were yielded with a 58–300 bp length range. Of these TDFs, 48 were isolated, cloned and sequenced. After trimming adapter sequences and removing redundant sequences, a total of 43 TDFs were obtained. Because the relatively limited knowledge of gene functions was found in *P. chrysosporium*, only 23 TDFs sequences displayed significant similarities to genes encoding known or predicted proteins, and the other 20 TDFs did not show significant matches, as determined by BLAST search (Tables 2 and 3). The results revealed 10, 4, and 5 significantly up-regulated TDFs in *P. chrysosporium* in response to 2, 8, and 24 h of Pb exposure respectively compared with 0 h of that, as well as 1, 4, and 3 significantly down-regulated TDFs (Table 2). The 8 h of Pb exposure to 50 and 400 mg L^{-1} Pb caused a significant up-regulation of 4 and 9 genes in *P. chrysosporium* compared with no exposure, and a significant down-regulation of 10 and 2 genes (Table 3).

3.3. Functional analysis and classifications of differentially expressed TDFs

The differentially expressed TDFs were analyzed with Blast2GO program for functional annotation of the GO terms of differentially expressed fragments with two approaches: BLASTn against the expressed sequence tag database and BLASTx against the non-redundant NR protein database (Wheeler et al., 2007). The results revealed that 23 TDFs sequences had significant similarities to genes with known or putative functions and 20 TDFs did not show significant matches (Tables 2 and 3). Of the 23 TDFs, 26.1% were homologous to *Phanerochaete carnosa* and 13.0% to *Pseudomonas* sp.

GO assignments describe gene products based on their associated biological processes, molecular functions, and cellular components by Blast2GO (Fig. 2). Regarding the differentially expressed fragments responded to different Pb-exposure time, “cellular protein catabolic process” and “protein modification” were the GO terms most frequently encountered (25% for each) in the biological process annotations, “ion binding” (23%) was the majority of annotations in the molecular function, and the annotations for cellular components were related to mitochondrion (67%) and membrane (33%) (Fig. 2a). Concerning the differentially expressed fragments related to the dose of Pb, “signaling”, “ion binding” and “membrane” were the major annotations for the biological processes, molecular functions, and cellular components, respectively (Fig. 2b).

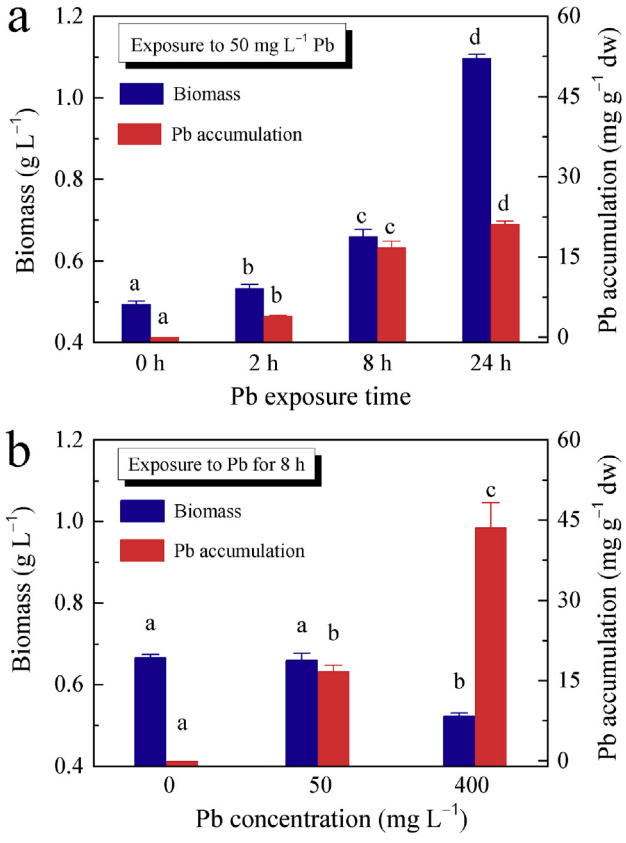

Fig. 1. The growth and metal accumulation of *P. chrysosporium* in exposure to Pb. (a) Effects of exposure time, (b) Effects of Pb concentration. The error bars represent standard deviation of three replicates. Different letters indicate significant differences ($P < 0.05$).

3.4. Gene expression analysis

HCA was conducted to group genes with similar expression profiles and the results displayed distinct clusters of putatively coexpressed TDFs (Fig. 3). At least six groups could be identified in *P. chrysosporium* in the case of different Pb-exposure time (Fig. 3a). For the six genes belonging to the Cluster I, an obvious up-regulation was observed after 2 h of Pb exposure, whereas 8 h and 24 h of that did not induce an obvious variation. Cluster II was characterized by an up-regulation after 8 h followed by a decline after 24 h. Two transcripts that were down-regulated after Pb treatment were grouped in the third cluster. Whereas Cluster IV including only one TDF identified as cysteine proteinase was characterized by a constant stimulation during 8 h of Pb exposure followed by a decline after 24 h. Cluster V holds together two transcripts that were down-regulated after 8 h of treatment. Finally, the TDF 13 that was identified as family sulfur acquisition oxidoreductase belonging to Cluster VI did not show a strong induction of its expression until 24 h of treatment.

Similarly, the differentially expressed TDFs responded to different Pb-dose exposures were arranged in three clusters (Fig. 3b). TDFs identified as TonB-dependent siderophore receptor, uroporphyrin-III methyltransferase and hypothetical protein were grouped in the first cluster, with their expression down-regulated in 50 mg L^{-1} Pb for 8 h. Cluster II contained a P-loop containing nucleoside triphosphate hydrolase protein which was involved in hydrolysis of the beta-gamma phosphate bond of a bound nucleoside triphosphate, the expression of which was induced after Pb treatment. Finally, the TDF 7 identified as RNA helicase was grouped in Cluster III that was up-regulated after 50 mg L^{-1} Pb exposure.

3.5. qRT-PCR analysis of Pb-induced differentially expressed TDFs

To check the reliability of cDNA-AFLP assay and validate its expression profile, qRT-PCR analyses were performed for 6 TDFs. These TDFs were selected based on the significance of their expression patterns, as well as their putative physiological role, which were related to thaumatin (TDF 12–1), Pre-mRNA-splicing factor ATP-dependent RNA helicase (TDF 42–1), ATP-dependent DNA helicase (TDF 45–1), LAGLIDADG homing endonuclease (TDF 47–1), hypothetical protein (TDF 1-1) and Plasma membrane proteolipid 3 (TDF 15–1). As shown in Fig. 4, the qRT-PCR results were consistent with the expression profiles revealed by cDNA-AFLP (Tables 2 and 3), supporting the reliability of this technology.

Table 2
Homologies of differentially expressed TDFs with known protein using BLASTX along with their expression patterns in *P. chrysosporium* exposed to 50 mg L^{-1} Pb for 0, 2, 8, and 24 h.

TDF	Size (bp)	Homologous protein	Organism origin	Accession number	E-value	Identity (%)	Expression pattern [a] 0 h	2 h	8 h	24 h
45-1	115	ATP-dependent DNA helicase	*Phlebia centrifuga*	OKY69186	2.87E-02	78	□	■	□	□
9-2	250	ATP-dependent RNA helicase	*Grifola frondosa*	OBZ72622	1.13E-07	96	□	■	□	□
38-1	143	cysteine proteinase	*Phanerochaete carnosa*	XP_007395877	3.94E-21	100	□	■	■	□
10-1	202	diguanylate cyclase	*Pseudomonas fluorescens*	WP_003215593	6.11E-39	100	□	□	■	□
13-1	122	family sulfur acquisition oxidoreductase	*Pseudomonas syringae*	WP_052962899	4.76E-22	100	□	□	□	■
14-1	75	Glucose-1-phosphate adenylyltransferase	*Klebsiella pneumoniae*	CDL51895	3.31E-07	100	■	■	□	■
43-2	154	hypothetical protein	*Phanerochaete carnosa*	XP_007402889	6.11E-04	59	□	■	□	□
34-1	112	hypothetical protein	*Phanerochaete carnosa*	XP_007394495	1.28E-12	89	■	■	□	■
47-1	134	LAGLIDADG homing endonuclease	*Lentinula edodes*	YP_006576301	8.51E-08	81	■	■	□	□
41-1	104	metallopeptidase	*Schizophyllum commune*	XP_003033858	5.20E-03	100	■	□	□	□
44-1	127	predicted protein	*Fibroporia radiculosa*	XP_012179232	1.71E-05	85	□	□	■	□
42-1	248	Pre-mRNA-splicing factor ATP-dependent RNA helicase	*Phanerochaete carnosa*	XP_007389812	6.66E-27	78	□	□	■	□
12-1	149	Thaumatin	*Fomitopsis pinicola*	EPT01966	1.09E-16	86	□	■	□	□
27-1	194	type I secretion C-terminal target domain-containing	*Acinetobacter gerneri*	EPR80393	4.70E-10	66	□	■	□	□
39-3	92	Ubiquitin carboxyl-terminal hydrolase 21	*Hypsizygus marmoreus*	KYQ43500	7.38E-10	97	□	■	□	□

[a] □, gene gel band absent or faint; ■, gene gel band visible; ■, gene gel bold bands.

Table 3
Homologies of differentially expressed TDFs with known protein using BLASTX along with their expression patterns in *P. chrysosporium* exposed to 0, 50, and 400 mg L^{-1} Pb for 8 h.

TDF	Size (bp)	Homologous protein	Organism origin	Accession number	E-value	Identity (%)	Expression pattern [a] 0	50	400
1-1	182	hypothetical protein	*Phanerochaete carnosa*	XP_007395324	1.48E-11	91	□	■	■
32-2	112	hypothetical protein	*Phanerochaete carnosa*	XP_007394495	1.28E-12	89	■	□	■
33-4	105	hypothetical protein	*Sphingomonas sp.*	WP_055780539	1.13E-07	82	□	□	■
15-1	111	Plasma membrane proteolipid 3	*Phialophora attae*	XP_007372289	2.49E-04	100	□	□	■
5-3	80	P-loop containing nucleoside triphosphate hydrolase protein	*Trametes versicolor*	XP_008033242	7.89E-07	92	□	□	■
7-2	154	RNA helicase	*Fomitiporia mediterranea*	XP_007267571	7.58E-17	100	■	■	■
16-2	107	TonB-dependent siderophore receptor	*Pseudomonas sp.*	WP_087694369	1.36E-15	100	■	□	■
19-1	74	uroporphyrin-III methyltransferase	*Marinobacter sp.*	WP_016669305	3.61E-07	92	■	□	■

[a] □, gene gel band absent or faint; ■, gene gel band visible; ■, gene gel bold bands; 0, 50 and 400 represents the concentration of Pb (mg L^{-1}).

4. Discussion

Pb contamination in the environment is known to cause adverse effects in humans and wildlife by damaging the nervous system and causing brain disorders (Huang et al., 2008; Li et al., 2016; Zeng et al., 2017). As an effective and economical alternative, biological means such as the utilization of *P. chrysosporium* through biosorption and uptake has been widely used for the treatment of Pb-contaminated wastewater (Huang et al., 2017d; Ye et al., 2017; Zeng et al., 2015). In spite of the rich data on the physiological and biochemical effects of Pb on *P. chrysosporium*, limited information is available at the molecular level. So, this study employed transcriptomics to explore the molecular mechanisms of Pb hyperaccumulation in *P. chrysosporium*.

4.1. Tolerance of P. chrysosporium to Pb exposure

Before identification and characterization of Pb-modulated genes in *P. chrysosporium*, we investigated the fungus growth and metal bioaccumulation in response to different exposure time and dose of Pb. The results indicated that *P. chrysosporium* displayed an outstanding resistant capacity to 50 mg L^{-1} Pb exposure, and could survive in a concentration of 400 mg L^{-1} Pb although an obvious inhibition on the growth was observed (Fig. 1). This could be ascribed to the defense mechanism of *P. chrysosporium* against Pb toxicity, mainly based on surface adsorption to polysaccharides, proteins or other components in the outer layer of the cell wall and uptake intracellularly (Li et al., 2015). Heavy metals that enter into the cell will pose a potential threat to fungi by directly increasing the concentration of reactive oxygen species (ROS). To alleviate the oxidative stress caused by enhanced ROS production, *P. chrysosporium* has evolved an antioxidant system consisting of enzymatic and non-enzymatic antioxidants (Huang et al., 2017a). In this study, high dose of Pb (400 mg L^{-1}) greatly induced the Pb accumulation in *P. chrysosporium*, and thus might contribute to the damage of cell membranes which accounted for the growth inhibition of fungus. Nevertheless, our results reveal that *P. chrysosporium* is effective in Pb bioaccumulation and is a promising alternative for the treatment of Pb-contaminated wastewater. The identification and characterization of the genes involved in Pb

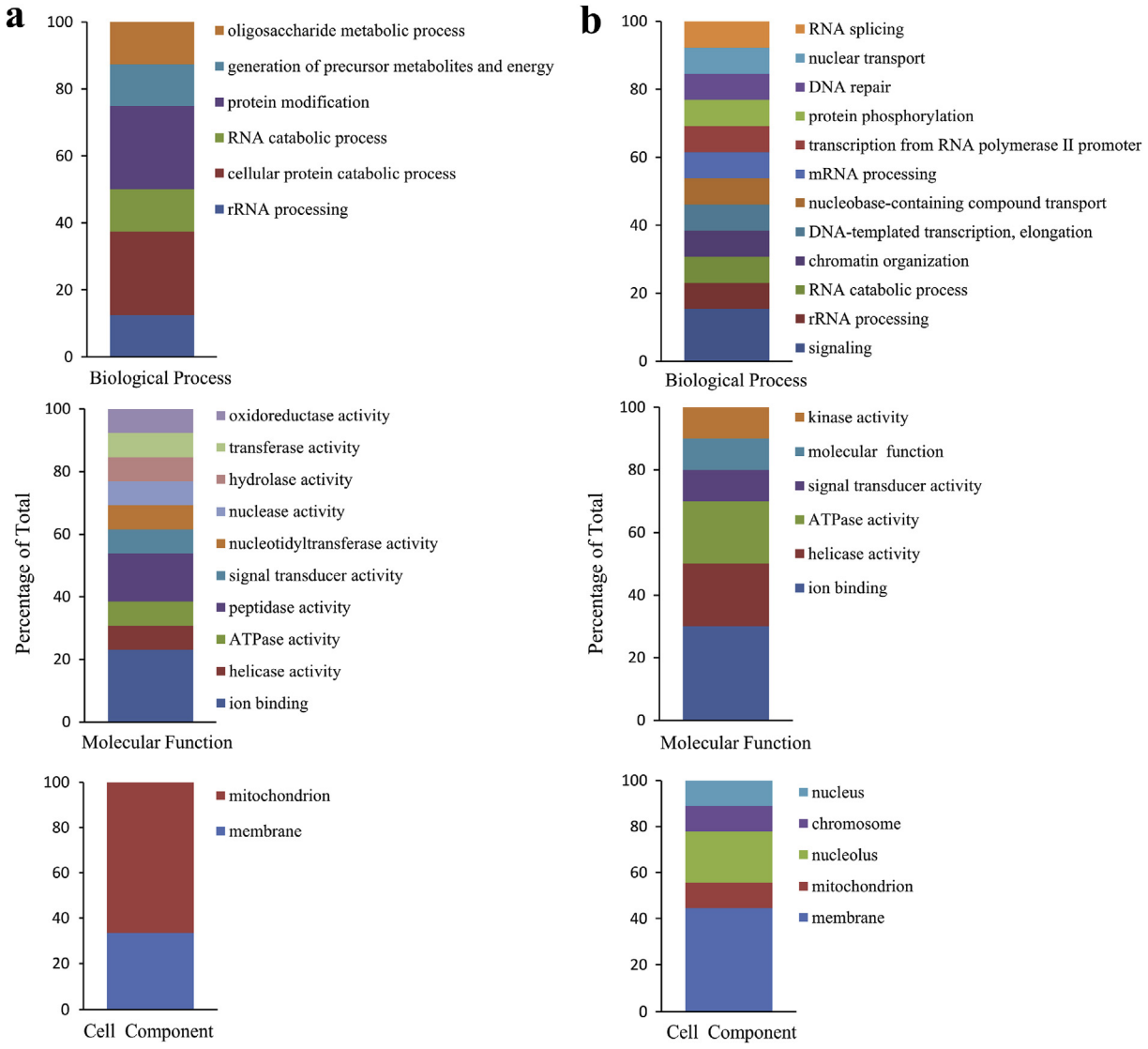

Fig. 2. Gene ontology classification of differentially expressed fragments in *P. chrysosporium* (a) treated with 50 mg L^{-1} Pb for 0, 2, 8, and 24 h, (b) treated with 0, 50, and 400 mg L^{-1} Pb for 8 h based on the annotation with Blast2GO.

tolerance and detoxification in *P. chrysosporium* can provide a potential basis for enhancement of the treatment performance.

4.2. Influence of Pb exposure on transcriptome

In this work, the modulation of transcriptional activity in *P. chrysosporium* exposed to different levels of Pb was ascertained by cDNA-AFLP, providing a comparative insight on potential Pb-regulated genes and metabolic pathways. After assembling and elimination, a total of 43 TDFs were obtained for annotation analysis. Of the 43 transcripts, 23 had significant homology to proteins in various functional categories when searching the non-redundant protein database, which made them the valuable information for understanding molecular mechanism in the Pb-fungus interaction. The 23 TDFs were classified based on Gene Ontology terms by Blast2GO. In terms of the biological process, a variety of annotations were attributed to 'metabolic processes' such as DNA repair, RNA catabolic process, and rRNA processing, indicating that Pb exposure posed an effect on the primary metabolism of *P. chrysosporium* by acting on the gene transcription. Regarding the molecular function, the transcripts involved in ion binding protein and ATPase activity were significantly represented, the result supports the previous studies concerning the fungal defense against heavy metal, reporting that the extracellular carboxylic and thiol groups played an important role in Pb detoxification through binding (Li et al., 2015; Xu et al., 2014).

qRT-PCR validation results showed that the expression patterns of selected genes were consistent with that observed in cDNA-AFLP, confirming that the use of cDNA-AFLP together with qRT-PCR validation is a reliable strategy to obtain the 'true' differentially expressed transcripts in *P. chrysosporium* exposed to Pb.

4.3. Potential target genes involved in defense mechanism

In recent years, several efforts have been devoted to the molecular mechanism behind the heavy metal tolerance of hyperaccumulators along with its potential genes for photoremediation, however, the related studies on fungi are limited. In the present work, twenty three genes as well as their role have been identified in fungus *P. chrysosporium* in response to Pb exposure. They are attributed to ion binding, energy and carbohydrate metabolism, signal transduction, and so on, according to the GO category of

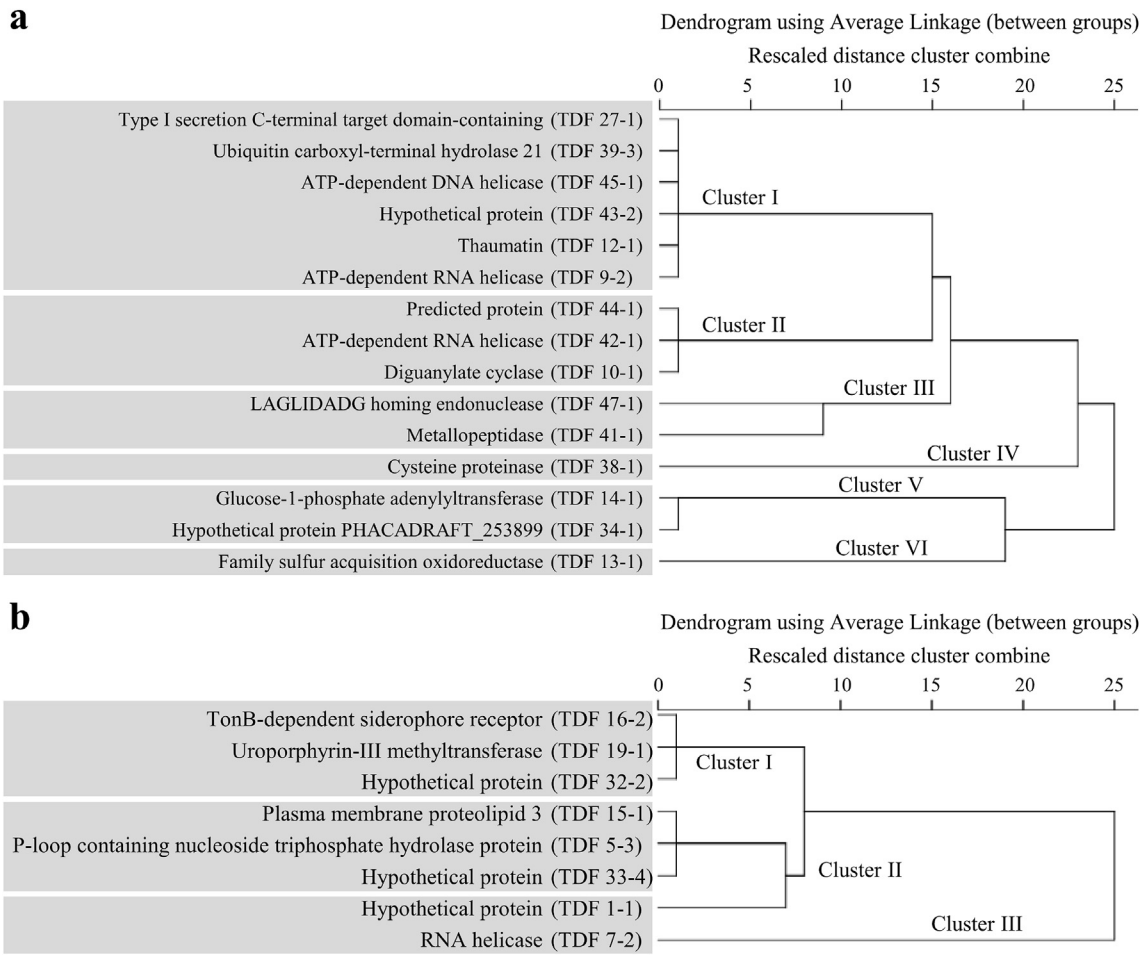

Fig. 3. Average linkage hierarchical cluster analysis (HCA) based on the expression patterns of TDFs from *P. chrysosporium* (a) exposed to 50 mg L^{-1} Pb for 0, 2, 8, and 24 h, (b) exposed to 0, 50, and 400 mg L^{-1} Pb for 8 h.

molecular function by Blast2GO.

Extracellular chelation through binding onto cell-wall components, which can contribute to the reduced uptake of metals into the cytosol, is known as an important tolerance mechanism to heavy metals in fungi (Ruytinx et al., 2011). In addition, several metal-binding proteins have been shown to function in the microbial heavy metal detoxification system, such as the periplasmic mercury-binding protein MerP (Desilva et al., 2002) and the periplasmic nickel-binding protein NikA (Nies, 1999). Herein, we isolated four up-regulated TDFs (5–3, 7–2, 9–2, 13–1) and two down-regulated TDFs (14–1, 16–2) related to ion binding (GO: 0043167), which accounted for a majority of annotations in molecular function, suggesting that ion binding might play a role in Pb tolerance. However, we found that metallopeptidase (TDF 41–1) was repressed in *P. chrysosporium* after exposure to 50 mg L^{-1} Pb for 2–24 h (Table 2), implying that metallopeptidase was down-regulated in response to Pb toxicity and it might not play an important role in defense against Pb stress. The same result was observed in other heavy metals such as chromium (Cammarota et al., 2006) and arsenic (Zheng et al., 2003).

ATPase plays key roles in cell energy metabolism by synthesizing ATP (Wu et al., 2014) and functions in diverse cellular processes such as DNA replication and cell cycle regulation (Snider et al., 2008). The uptake of heavy metals by cell often uses ATP hydrolysis as the energy source (Nies, 1999). Zhou et al. (2017) observed that manganese up-regulated and down-regulated AAA-type ATPase family protein (NP_197195.2) in *Citrus grandis* and *Citrus sinensis*, respectively. We found that three TDFs (5–3, 7–2, 9–2) related to ATPase activity (GO: 0016887) were all up-regulated in response to different dose (50–400 mg L^{-1}) or time (2–24 h) of Pb exposure, indicating that ATPase was involved in tolerance of *P. chrysosporium* to Pb. In addition, we identified another two up-regulated TDFs, TDF 42–1 and 45–1, which were recognized as ATP-dependent RNA/DNA helicase and related to nucleic acid metabolism, and the qRT-PCR analysis validated the expression of the two genes whose expression level was significantly higher after 8 h (TDF 42–1) and 2 h (TDF 45–1) of Pb exposure than that at 0 h.

Besides, it was found that the expression of TDFs (5–3, 10–1) related to signal transduction was altered in Pb-toxic *P. chrysosporium*. TDF 5–3 was recognized as P-loop containing nucleoside triphosphate hydrolase protein (Table 3), which was reported to be involved in diverse cellular functions, such as signal transduction, DNA repair, protein transport and localization, signal-sequence recognition, membrane transport and activation of various metabolites (Pathak et al., 2014). The stress of 400 mg L^{-1} Pb significantly induced the expression of TDF 5–3, while 50 mg L^{-1} Pb did not, with respect to the control without Pb stress, suggesting that TDF 5–3 was a potential biomarker for high concentration of Pb in *P. chrysosporium*.

Transport process was also altered in *P. chrysosporium* exposed to Pb, as evidenced by Pb-toxicity-responsive TDF 14–1 related to cellular transport. Several metal-transporters have been identified in the transport of arsenic, aluminum and zinc (Jacobs et al., 2002; Ovečka and Takáč, 2014). Glucose-1-phosphate adenylyltransferase

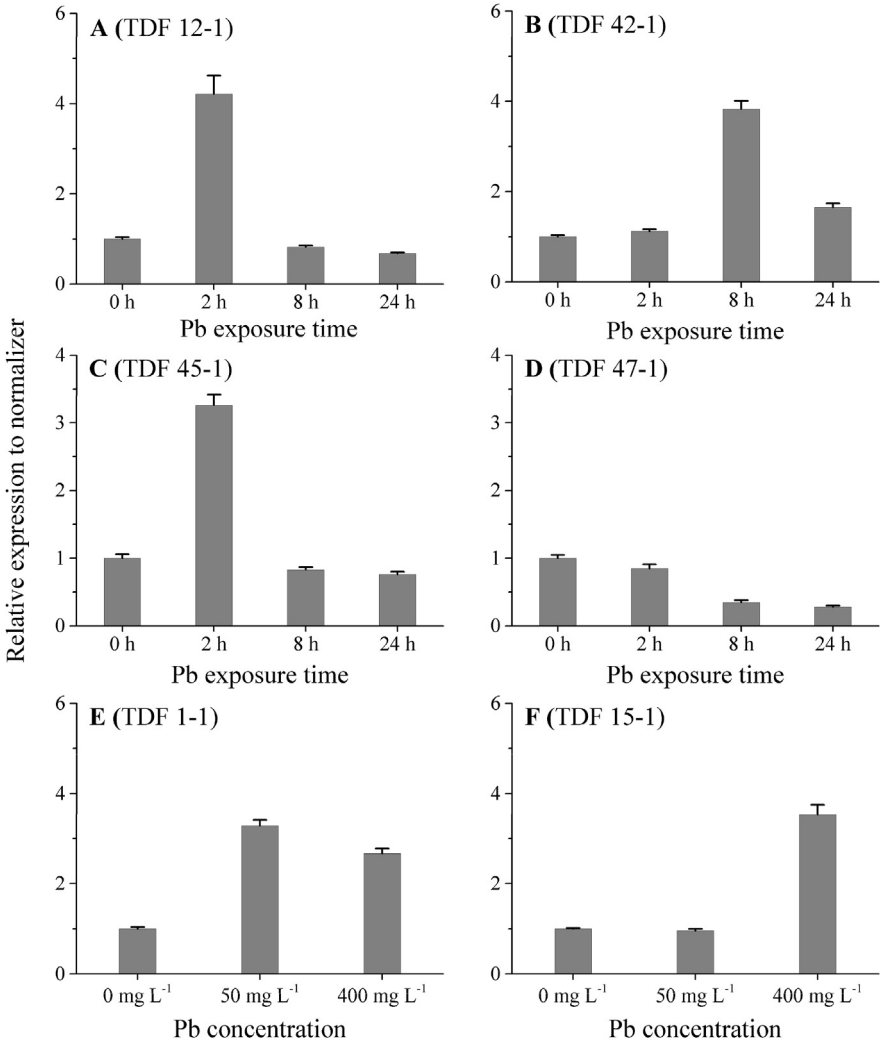

Fig. 4. Relative expression of TDFs from *P. chrysosporium* in exposure to Pb. (A–D) Effects of exposure time at a Pb concentration of 50 mg L^{-1}, (E–F) Effects of Pb concentration after 8 h of exposure. The error bars represent standard deviation of three replicates.

(TDF 14–1) belongs to the family of transferases, specifically those transferring phosphorus-containing nucleotide groups. Interestingly, it was down-regulated only after 8 h of 50 mg L^{-1} Pb exposure in *P. chrysosporium* (Table 2) and the reason might be attributed to the influence on gene expression at post-transcriptional level (Mazzucotelli et al., 2008).

5. Conclusion

P. chrysosporium constitutes an interesting species for studying heavy metal stress response in fungi, and also for bioremediation applications in contaminated wastewater and soil. Our studies about *P. chrysosporium* in response to Pb highlighted its outstanding ability in Pb tolerance and effective defense system. By using cDNA-AFLP, we isolated 48 differentially expressed TDFs from *P. chrysosporium* exposed to Pb, and 23 TDFs showed significant homology with proteins in different functional categories, such as ion binding, energy and carbohydrate metabolism, and signal transduction. The detailed characterization of these Pb-responsive genes, which presented to be involved in specific processes, will help to reveal the molecular mechanisms and regulatory networks responsible for heavy metal accumulation and tolerance in *P. chrysosporium*. However, about 46% of the identified genes did not show significant similarities to genes with known or putative functions, which might also be involved in its tolerance and needed further exploration. Our data provide a global view of differential gene expression in *P. chrysosporium* exposed to Pb, and could serve as fundamental research clues for further studies, especially provide potential targets for the improvement in bioremediation capacity of *P. chrysosporium*.

Acknowledgments

This study was financially supported by the Program for the National Natural Science Foundation of China (51579098, 51779090, 51709101, 51278176, 51408206, 51521006), the National Program for Support of Top–Notch Young Professionals of China (2014), Hunan Provincial Science and Technology Plan Project (No.2016RS3026), and the Program for Changjiang Scholars and Innovative Research Team in University (IRT-13R17).

References

Brockmeier, E.K., Scott, P.D., Denslow, N.D., Leusch, F.D.L., 2016. Transcriptomic and physiological changes in Eastern Mosquitofish (*Gambusia holbrooki*) after exposure to progestins and anti-progestagens. Aquat. Toxicol. 179, 8–17.

Cammarota, M., Lamberti, M., Masella, L., Galletti, P., De Rosa, M., Sannolo, N., et al., 2006. Matrix metalloproteinases and their inhibitors as biomarkers for metal toxicity in vitro. Toxicol. in Vitro 20, 1125–1132.

Chen, A.W., Zeng, G.M., Chen, G.Q., Liu, L., Shang, C., Hu, X.J., et al., 2014. Plasma membrane behavior, oxidative damage, and defense mechanism in *Phanerochaete chrysosporium* under cadmium stress. Process Biochem. 49, 589–598.
Conesa, A., Götz, S., García-Gómez, J.M., Terol, J., Talón, M., Robles, M., 2005. Blast2GO: a universal tool for annotation, visualization and analysis in functional genomics research. Bioinformatics 21, 3674–3676.
Desilva, T.M., Veglia, G., Porcelli, F., Prantner, A.M., Opella, S.J., 2002. Selectivity in heavy metal - binding to peptides and proteins. Biopolymers 64, 189–197.
Georgieva, T., Christov, N.K., Djilianov, D., 2012. Identification of desiccation-regulated genes by cDNA-AFLP in *Haberlea rhodopensis*: a resurrection plant. Acta Physiol. Plant. 34, 1055–1066.
Gong, X.M., Huang, D.L., Liu, Y.G., Zeng, G.M., Wang, R.Z., Wan, J., et al., 2017. Stabilized nanoscale zerovalent iron mediated cadmium accumulation and oxidative damage of *Boehmeria nivea* (L.) Gaudich cultivated in cadmium contaminated sediments. Environ. Sci. Technol. 51, 11308–11316.
Gutiérrez, M., Rojas, L.A., Mancilla-Villalobos, R., Seelenfreund, D., Vicuña, R., Lobos, S., 2008. Analysis of manganese-regulated gene expression in the ligninolytic basidiomycete *Ceriporiopsis subvermispora*. Curr. Genet. 54, 163.
Hiki, K., Nakajima, F., Tobino, T., 2017. Application of cDNA-AFLP to biomarker exploration in a non-model species *Grandidierella japonica*. Ecotoxicol. Environ. Saf. 140, 206–213.
Huang, C., Lai, C., Xu, P., Zeng, G.M., Huang, D.L., Zhang, J.C., et al., 2017a. Lead-induced oxidative stress and antioxidant response provide insight into the tolerance of *Phanerochaete chrysosporium* to lead exposure. Chemosphere 187, 70–77.
Huang, C., Lai, C., Zeng, G.M., Huang, D.L., Xu, P., Zhang, C., et al., 2017b. Manganese-enhanced degradation of lignocellulosic waste by *Phanerochaete chrysosporium*: evidence of enzyme activity and gene transcription. Appl. Microbiol. Biotechnol. 101, 6541–6549.
Huang, C., Zeng, G.M., Huang, D.L., Lai, C., Xu, P., Zhang, C., et al., 2017c. Effect of *Phanerochaete chrysosporium* inoculation on bacterial community and metal stabilization in lead-contaminated agricultural waste composting. Bioresour. Technol. 243, 294–303.
Huang, D.L., Hu, C.J., Zeng, G.M., Cheng, M., Xu, P., Gong, X.M., et al., 2017d. Combination of Fenton processes and biotreatment for wastewater treatment and soil remediation. Sci. Total. Environ 574, 1599–1610.
Huang, D.L., Qin, X.M., Xu, P., Zeng, G.M., Peng, Z.W., Wang, R.Z., et al., 2016a. Composting of 4-nonylphenol-contaminated river sediment with inocula of *Phanerochaete chrysosporium*. Bioresour. Technol. 221, 47–54.
Huang, D.L., Xue, W.J., Zeng, G.M., Wan, J., Chen, G.M., Huang, C., et al., 2016b. Immobilization of Cd in river sediments by sodium alginate modified nanoscale zero-valent iron: impact on enzyme activities and microbial community diversity. Water Res. 106, 15–25.
Huang, D.L., Zeng, G.M., Feng, C.L., Hu, S., Jiang, X.Y., Tang, L., et al., 2008. Degradation of lead-contaminated lignocellulosic waste by *Phanerochaete chrysosporium* and the reduction of lead toxicity. Environ. Sci. Technol. 42, 4946–4951.
Jacobs, D.E., Clickner, R.P., Zhou, J.Y., Viet, S.M., Marker, D.A., Rogers, J.W., et al., 2002. The prevalence of lead-based paint hazards in US housing. Environ. Health Persp. 110. A599.
Jia, F., Lai, C., Chen, L., Zeng, G.M., Huang, D.L., Liu, F., et al., 2017. Spatiotemporal and species variations in prokaryotic communities associated with sediments from surface-flow constructed wetlands for treating swine wastewater. Chemosphere 185, 1–10.
Jiang, X., Qiu, L.G., Zhao, H.W., Song, Q.Q., Zhou, H.L., Han, Q., Diao, X.P., 2016. Transcriptomic responses of *Perna viridis* embryo to Benzo(a)pyrene exposure elucidated by RNA sequencing. Chemosphere 163, 125–132.
Lai, C., Wang, M.M., Zeng, G.M., Liu, Y.G., Huang, D.L., Zhang, C., et al., 2016. Synthesis of surface molecular imprinted TiO2/graphene photocatalyst and its highly efficient photocatalytic degradation of target pollutant under visible light irradiation. Appl. Surf. Sci. 390, 368–376.
Li, N.J., Zeng, G.M., Huang, D.L., Huang, C., Lai, C., Wei, Z., et al., 2015. Response of extracellular carboxylic and thiol ligands (oxalate, thiol compounds) to Pb^{2+} stress in *Phanerochaete chrysosporium*. Environ. Sci. Pollut. R 22, 12655–12663.
Li, X.M., Peng, W.H., Jia, Y.Y., Lu, L., Fan, W.H., 2016. Bioremediation of lead contaminated soil with *Rhodobacter sphaeroides*. Chemosphere 156, 228–235.
Livak, K.J., Schmittgen, T.D., 2001. Analysis of relative gene expression data using real-time quantitative PCR and the $2^{-\Delta\Delta CT}$ method. Methods 25, 402–408.
Mazzucotelli, E., Mastrangelo, A.M., Crosatti, C., Guerra, D., Stanca, A.M., Cattivelli, L., 2008. Abiotic stress response in plants: when post-transcriptional and post-translational regulations control transcription. Plant Sci. 174, 420–431.
Neale, P.A., Achard, M.E.S., Escher, B.I., Leusch, F.D.L., 2017. Exploring the oxidative stress response mechanism triggered by environmental water samples. Environ. Sci. Proc. Impacts 19, 1126–1133.
Nies, D.H., 1999. Microbial heavy-metal resistance. Appl. Microbiol. Biotechnol. 51, 730–750.
Oberholster, P.J., Hill, L., Jappie, S., Truter, J.C., Botha, A.M., 2016. Applying genotoxicology tools to identify environmental stressors in support of river management. Chemosphere 144, 319–329.
Ovečka, M., Takáč, T., 2014. Managing heavy metal toxicity stress in plants: biological and biotechnological tools. Biotechnol. Adv. 32, 73–86.
Pathak, E., Atri, N., Mishra, R., 2014. Analysis of P-loop and its flanking region subsequence of diverse NTPases reveals evolutionary selected residues. Bioinformation 10, 216.
Petr, B., 2003. Interactions of heavy metals with white-rot fungi. Enzyme Microb. Tech 32, 78–91.
Ren, X.Y., Zeng, G.M., Tang, L., Wang, J.J., Wan, J., Feng, H.P., et al., 2018. Effect of exogenous carbonaceous materials on the bioavailability of organic pollutants and their ecological risks. Soil Biol. Biochem. 116, 70–81.
Ruytinx, J., Craciun, A., Verstraelen, K., Vangronsveld, J., Colpaert, J., Verbruggen, N., 2011. Transcriptome analysis by cDNA-AFLP of *Suillus luteus* Cd-tolerant and Cd-sensitive isolates. Mycorrhiza 21, 145–154.
Snider, J., Thibault, G., Houry, W.A., 2008. The AAA+ superfamily of functionally diverse proteins. Genome Biol. 9, 216.
Vidal-Dorsch, D.E., Bay, S.M., Moore, S., Layton, B., Mehinto, A.C., Vulpe, C.D., et al., 2016. Ecotoxicogenomics: microarray interlaboratory comparability. Chemosphere 144, 193–200.
Vos, P., Hogers, R., Bleeker, M., Reijans, M., Van De Lee, T., Hornes, M., et al., 1995. AFLP: a new technique for DNA fingerprinting. Nucleic Acids Res. 23, 4407–4414.
Vuylsteke, M., Peleman, J.D., Van Eijk, M.J., 2007. AFLP-based transcript profiling (cDNA-AFLP) for genome-wide expression analysis. Nat. Protoc. 2, 1399–1413.
Wan, J., Zeng, G.M., Huang, D.L., Hu, L., Xu, P., Huang, C., et al., 2018. Rhamnolipid stabilized nano-chlorapatite: synthesis and enhancement effect on Pb-and Cd-immobilization in polluted sediment. J. Hazard. Mater 343, 332–339.
Wang, H., Yuan, X.Z., Wu, Y., Chen, X.H., Leng, L.J., Wang, H., et al., 2015a. Facile synthesis of polypyrrole decorated reduced graphene oxide–Fe_3O_4 magnetic composites and its application for the Cr(VI) removal. Chem. Eng. J. 262, 597–606.
Wang, H., Yuan, X.Z., Wu, Y., Huang, H.J., Zeng, G.M., Liu, Y., et al., 2013. Adsorption characteristics and behaviors of graphene oxide for Zn(II) removal from aqueous solution. Appl. Surf. Sci. 279, 432–440.
Wang, H., Yuan, X.Z., Wu, Y., Zeng, G.M., Chen, X.H., Leng, L.J., et al., 2015b. Facile synthesis of amino-functionalized titanium metal-organic frameworks and their superior visible-light photocatalytic activity for Cr(VI) reduction. J. Hazard. Mater 286, 187–194.
Wheeler, D.L., Barrett, T., Benson, D.A., Bryant, S.H., Canese, K., Chetvernin, V., et al., 2007. Database resources of the national center for biotechnology information. Nucleic Acids Res. 36, D13–D21.
Wu, Q., Andrianaivomananjaona, T., Tetaud, E., Corvest, V., Haraux, F., 2014. Interactions involved in grasping and locking of the inhibitory peptide IF1 by mitochondrial ATP synthase. BBA-Bioenergetics 1837, 761–772.
Xu, P., Liu, L., Zeng, G.M., Huang, D.L., Lai, C., Zhao, M.H., et al., 2014. Heavy metal-induced glutathione accumulation and its role in heavy metal detoxification in *Phanerochaete chrysosporium*. Appl. Microbiol. Biotechnol. 98, 6409–6418.
Xu, P., Zeng, G.M., Huang, D.L., Liu, L., Zhao, M.H., Lai, C., et al., 2016. Metal bioaccumulation, oxidative stress and antioxidant defenses in *Phanerochaete chrysosporium* response to Cd exposure. Ecol. Eng. 87, 150–156.
Xu, P., Zeng, G.M., Huang, D.L., Feng, C.L., Hu, S., Zhao, M.H., et al., 2012a. Use of iron oxide nanomaterials in wastewater treatment: a review. Sci. Total. Environ 424, 1–10.
Xu, P., Zeng, G.M., Huang, D.L., Lai, C., Zhao, M.H., Wei, Z., et al., 2012b. Adsorption of Pb(II) by iron oxide nanoparticles immobilized *Phanerochaete chrysosporium*: equilibrium, kinetic, thermodynamic and mechanisms analysis. Chem. Eng. J. 203, 423–431.
Yang, C.P., Chen, H., Zeng, G.M., Yu, G.L., Luo, S.L., 2010. Biomass accumulation and control strategies in gas biofiltration. Biotechnol. Adv. 28, 531–540.
Ye, S.J., Zeng, G.M., Wu, H.P., Zhang, C., Dai, J., Liang, J., et al., 2017. Biological technologies for the remediation of co-contaminated soil. Crit. Rev. Biotechnol. 37, 1062–1076.
Yu, Z.G., Zhang, C., Zheng, Z.H., Hu, L., Li, X.M., Yang, Z.Z., et al., 2017. Enhancing phosphate adsorption capacity of SDS-based magnetite by surface modification of citric acid. Appl. Surf. Sci. 403, 413–425.
Zeng, G.M., Chen, M., Zeng, Z.T., 2013a. Risks of neonicotinoid pesticides. Science 340, 1403, 1403.
Zeng, G.M., Chen, M., Zeng, Z.T., 2013b. Shale gas: surface water also at risk. Nature 499, 154, 154.
Zeng, G.M., Li, N.J., Huang, D.L., Lai, C., Zhao, M.H., Huang, C., et al., 2015. The stability of Pb species during the Pb removal process by growing cells of *Phanerochaete chrysosporium*. Appl. Microbiol. Biotechnol. 99, 3685–3693.
Zeng, G.M., Wan, J., Huang, D.L., Hu, L., Huang, C., Cheng, M., et al., 2017. Precipitation, adsorption and rhizosphere effect: the mechanisms for Phosphate-induced Pb immobilization in soils—a review. J. Hazard. Mater 339, 354–367.
Zhang, C., Yu, Z.G., Zeng, G.M., Huang, B.B., Dong, H.R., Huang, J.H., et al., 2016. Phase transformation of crystalline iron oxides and their adsorption abilities for Pb and Cd. Chem. Eng. J. 284, 247–259.
Zhang, C., Yu, Z.G., Zeng, G.M., Jiang, M., Yang, Z.Z., Cui, F., et al., 2014. Effects of sediment geochemical properties on heavy metal bioavailability. Environ. Int. 73, 270–281.
Zhao, M.H., Zhang, C.S., Zeng, G.M., Huang, D.L., Xu, P., Cheng, M., 2015. Growth, metabolism of Phanerochaete chrysosporium and route of lignin degradation in response to cadmium stress in solid-state fermentation. Chemosphere 138, 560–567.
Zheng, X.H., Watts, G.S., Vaught, S., Gandolfi, A.J., 2003. Low-level arsenite induced gene expression in HEK293 cells. Toxicology 187, 39–48.
Zhou, C.P., Li, C.P., Liang, W.W., Guo, P., Yang, L.T., Chen, L.S., 2017. Identification of manganese-toxicity-responsive genes in roots of two citrus species differing in manganese tolerance using cDNA-AFLP. Trees 31, 813–831.